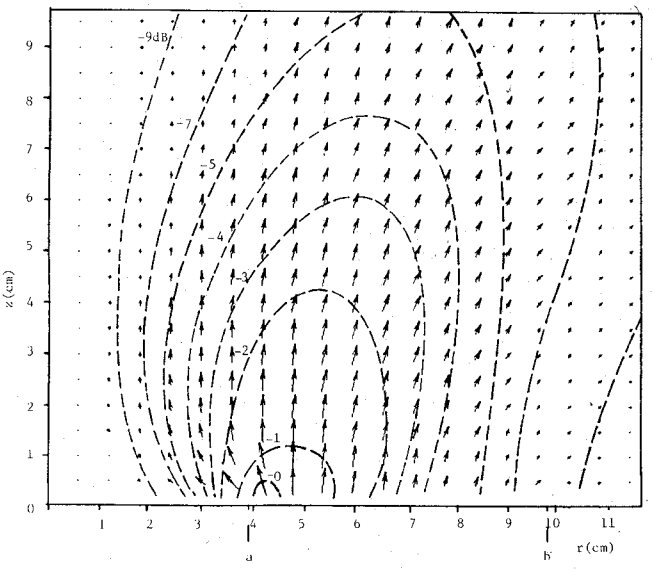

Fig. 7. Constant time-average power density patterns and power flow directions when the exterior region is air, $b/a = 2.5$, and $ka = 2.0$.

the center conductor. At distances several wavelengths from the center of the annular aperture, the power flow turns toward the radial direction. Contours of constant power flux density appear as dashed lines in Fig. 7. An expected null exists on the vertical center axis due to the interaction of fields on opposite sides of the annular ring.

The addition of higher order reflected modes has been observed to have little effect on the input admittance. Virtually no difference is observed between the input admittance results for the two approaches (with or without higher order interior modes) when the exterior region is composed of fat or bone and muscle. These are cases where, in the exterior region, the aperture size is less than 2.5 wavelengths and the medium is lossy. As long as the aperture size remains less than 2.5 wavelengths in the exterior medium, the lack of an effect by the higher order modes on the input admittance tends to support previous work [11] which relies solely on TEM modes to determine the dielectric constant of materials in the exterior region.

References

[1] H. Levine and C. H. Papas, "Theory of the circular diffraction antenna," *J. Appl. Phys.*, vol. 22, pp. 29–43, Jan. 1951.
[2] L. S. Taylor, "Electromagnetic syringe," *IEEE Trans. Bio-med. Eng.*, vol. BME-25, pp. 308–309, May 1978.
[3] M. L. Swicord and C. C. Davis, "Energy absorption from small radiating coaxial probes in lossy media," *IEEE Trans. Microwave Theory Tech.*, vol. MTT-29, pp. 1202–1209, Nov. 1981.
[4] I. J. Bahl and S. S. Stuchy, "The effect of finite size of the ground plane on the impedance of a monopole immersed in a lossy medium," *Electron. Lett.*, vol. 15, pp. 728–729, 1979.
[5] D. C. Chang, "Input admittance and complete near-field distribution of an annular aperture antenna driven by a coaxial line," *IEEE Trans. Antennas Propagat.*, vol. AP-18, pp. 610–616, Sept. 1970.
[6] E. P. Irzinski, "The input admittance of a TEM excited annular slot antenna," *IEEE Trans. Antennas Propagat.*, vol. AP-23, pp. 829–834, Nov. 1975.
[7] R. Harrington, *Field Computation by the Method of Moments*. New York: Macmillan, 1968.
[8] R. Harrington, *Time Harmonic Electromagnetic Fields*. New York: McGraw-Hill, 1961, ch. 3.
[9] C. M. Butler and L. L. Tsai, "An alternate frill field formulation," *IEEE Trans. Antennas Propagat.*, vol. AP-21, pp. 115–116, Jan. 1973.
[10] A. W. Guy, J. E. Lehmann, and J. B. Stonebridge, "Therapeutic applications of electromagnetic power," *Proc. IEEE*, vol. 62, pp. 55–75, Jan. 1974.
[11] E. C. Burdette, F. L. Cain, and J. Seals, "*In vivo* probe measurement technique for determining dielectric properties at VHF through microwave frequencies," *IEEE Trans. Microwave Theory Tech.*, vol. MTT-28, pp. 414–427, Apr. 1980.

Mathematical Expression of the Loading Characteristics of Microwave Oscillators and Injection-Locking Characteristics

KATSUMI FUKUMOTO, MASAMITSU NAKAJIMA, MEMBER, IEEE, AND JUN-ICHI IKENOUE

***Abstract*—Most of the studies concerning microwave oscillators have so far been based on the Van der Pol oscillator model. However, this model is too simple to obtain good agreement between observation and theory. Our previous paper proposed a new mathematical model which describes the loading characteristics of oscillators more accurately than the Van der Pol model does. In this paper, we have investigated injection-locked microwave oscillators using the mathematical model to find out the relation between the loading and injection-locking characteristics.**

I. Introduction

Many researchers have studied the loading characteristics and locking phenomena of oscillators in the low-frequency region, in which an oscillator circuit can be treated as a lumped-constant circuit [1]. In the microwave region, however, an oscillator circuit should be treated as a distributed-constant circuit. Although there is no essential difference in the oscillation phenomena between the two frequency regions [2], the characteristics of the oscillators appear to be different between the two regions. This is mainly because, in the case of injection-locking phenomena, the input and output signals are measured in terms of voltage or current in the low-frequency region, while in the microwave region, they are measured in terms of traveling waves. The differential equations which describe the relation between the input and output signals should be practically different between the two regions. However, when the magnitude of the input signal is small, the differential equations which describe the phase relation happen to be of the same form [3]. Distinction becomes apparent when the input signal is large, the differential equations assuming different forms. Obviously, it may be reasonable to treat microwave oscillators in terms of traveling waves.

In this paper, we will analyze large-signal injection-locking phenomena using the extended oscillator model with the concept of traveling waves. We will find out the relationship between the loading characteristics and the injection-locking characteristics of oscillators. This will give us an estimate of the validity of the numerical expression of oscillator characteristics, and the usefulness of the oscillator model will be demonstrated.

The theory is confirmed to be in good agreement with experiment.

Manuscript received January 4, 1984; revised October 30, 1984.

K. Fukumoto is with the Semiconductor Research Laboratories, Sharp Corporation, Tenri, Nara, Japan.
M. Nakajima and J. Ikenoue are with the Department of Electronics, Kyoto University, Kyoto, Japan.

0018-9480/85/0400-0319$01.00 ©1985 IEEE

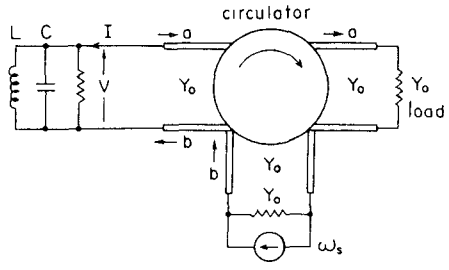

Fig. 1. Injection-locking of a microwave oscillator

II. Analysis of Injection-Locking Characteristics in Terms of Traveling Waves

A. Locking Equation

The oscillator admittance is given by a polynomial function of frequency and voltage [4]

$$Y(j\omega,|V|^2) = Y_n + Y_\omega \cdot \Delta\omega + Y_v \cdot |V|^2 + Y_{\omega 2} \cdot \Delta\omega^2 \tag{1}$$

where

$$\begin{aligned} &Y_n = -G_0 + jB_0,\ Y_\omega = G_\omega + jB_\omega, \\ &Y_v = G_v + jB_v,\ Y_{\omega 2} = G_{\omega 2} + jB_{\omega 2} \\ &\Delta\omega = \omega - \omega_0 \end{aligned} \tag{2}$$

and ω_0 is the free-running angular frequency.

With the admittance (1), the equation describing the voltage phase and amplitude behavior of an oscillator is written [3]

$$I = \left\{ Y(j\omega,|V|^2) + Y_{j\omega} \cdot d/dt \right\} V \tag{3}$$

where $Y_{j\omega} = \partial Y/\partial(j\omega)$.

In the case of the free-running steady state ($d/dt = 0$) where the oscillator is connected (as shown in Fig. 1) to a transmission line (characteristic admittance Y_0) with no signal injected, (3) becomes

$$Y(j\omega_0,|V_0|^2) = I/V = -Y_0. \tag{4}$$

From this equation, the free-running voltage amplitude $|V_0|$ and frequency ω_0 is determined.

Let the deviation of amplitude from the free-running steady-state value be

$$\Delta|V| = |V| - |V_0|. \tag{5}$$

We expand $Y(j\omega,|V|^2)$ in a Taylor series in the neighborhood of the free-running state, and neglect higher order terms

$$Y(j\omega,|V|^2) = -Y_0 + Y_{j\omega 0} \cdot j\Delta\omega + Y_{|V_0|} \cdot \Delta|V| \tag{6}$$

where use is made of (4).

The emanating wave a and the incident wave b

$$a = |a|\exp(j\alpha), \quad b = |b|\exp(j\beta) \tag{7}$$

are related to the voltage V and I of the oscillator by the definition

$$V = (b+a)/\sqrt{Y_0}, \quad I = (b-a)\sqrt{Y_0}. \tag{8}$$

Substituting (3) and (8) into (6), we have the relation between a and b [3]. By solving it, we find the output power $|\hat{a}|^2$ as a function of the input power $|\hat{b}|^2$ into the oscillator, where $\hat{a}$ and $\hat{b}$ are normalized to the emanating wave amplitude $|a_0| = \sqrt{Y_0}|V_0|$ in the free-running state.

B. Stability Criterion

Substituting (8) into (3), and solving for da/dt, we obtain [3]

$$F = \frac{da}{dt} = \left\{ (b-a) \cdot Y_0 + (b+a) \cdot Y(j\omega,|V|^2) \right\} / Y_{j\omega}. \tag{9}$$

From Routh–Hurwitz' criterion, we get the following stability condition (Appendix I):

$$\begin{aligned} &\mathrm{Re}(\partial F/\partial a) < 0 \\ &|\partial F/\partial a|^2 > |\partial F/\partial a^*|^2. \end{aligned} \tag{10}$$

Therefore, the stability condition of the stationary state is obtained as

$$\mathrm{Re}\left[Y_{j\omega}^* \left\{ Y_0 + \sqrt{Y_0}|V_0|(\hat{b}+\hat{a}) \cdot Y_a + Y_0(2\hat{b}/(\hat{b}+\hat{a}) - 1) \right\} \right] > 0 \tag{11}$$

$$\begin{aligned} &|Y_0 + Y_a\sqrt{Y_0}|V_0|(\hat{b}+\hat{a}) + Y_0(2\hat{b}/(\hat{b}+\hat{a}) - 1)| \\ &\qquad > |Y_a^*\sqrt{Y_0}|V_0|(\hat{b}+\hat{a})|. \end{aligned} \tag{12}$$

III. Relation Between the Oscillator Admittance and the Injection-Locking Characteristics

Now we investigate the effects of the coefficients of (1) on the injection-locking characteristics. We refer to the Van der Pol oscillator model, the case where $Y_n = -G_0 (< 0)$, $Y_\omega = jB_\omega$, $Y_v = G_v$, and $Y_{\omega 2} = 0$ are satisfied, and we regard it as a reference model for the analysis that follows. In passing, the maximum output power of the Van der Pol oscillator is given by $P_{\max} = G_0^2/4G_v$ [4].

A. Injection-Locking Characteristics of the Van der Pol Oscillator

Fig. 2 shows the injection-locking characteristics of the Van der Pol oscillator. The oscillator used in the experiment produces the maximum output power when the load admittance is chosen as $G_0 = 2.36Y_0$. Since $G_0 > 2Y_0$ holds, the oscillator is loosely connected to a transmission line Y_0 so that the oscillator output power decreases monotonically as the injection signal increases in amplitude.

For the sake of numerical evaluation in what follows, we introduce the normalization as

$$\begin{aligned} Y(j\omega,|V|^2)/Y_0 &\equiv \hat{Y}(jx,|\hat{V}|^2) \\ &= \hat{Y}_n + \hat{Y}_\omega x + \hat{Y}_v|\hat{V}|^2 + \hat{Y}_{\omega 2}x^2 \\ \delta &= \frac{\omega - \omega_0}{\omega_0}, \qquad Q = \frac{\omega_0 B_\omega}{2Y_0}, \\ x &= 2\delta Q, \qquad |\hat{V}|^2 = |V|^2/|V_m|^2 \\ |V_m|^2 &= G_0/G_v \cdot 2, \qquad \hat{Y}_n = Y_n/Y_0, \\ \hat{Y}_\omega &= Y_\omega \cdot \omega_0/2\theta Y_0 \qquad \hat{Y}_v = Y_v|V_m|^2/Y_0, \\ \hat{Y}_{\omega 2} &= Y_{\omega 2} \cdot \omega_0^2/4\theta^2 Y_0, \qquad \hat{P} = |a|^2/P_{\max}. \end{aligned} \tag{13}$$

B. The Effect of the Coefficient G_ω

When the coefficient G_ω is added to the Van der Pol oscillator, it makes the amplitude characteristics of synchronization asymmetric with respect to frequency. The same is true for equi-power loci on the Rieke diagram. The effect becomes noticeable for $|\hat{G}_\omega| > 0.3$. This is because G_ω makes the negative resistance an odd function with respect to frequency deviation.

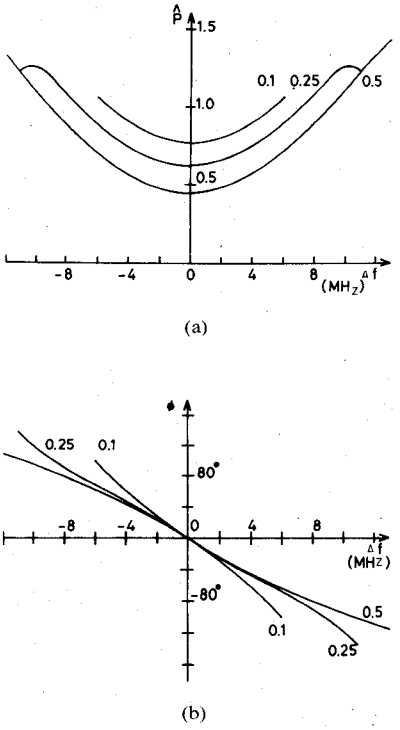

Fig. 2. Injection-locking characteristics of Van der Pol's oscillator. (Parameters: $|\hat{b}|^2$; $\hat{G}_0 = 2.36$, $\hat{G}_v = 1.18$, $\hat{B}_\omega = 1$.) (a) Amplitude characteristics. (b) Phase characteristics.

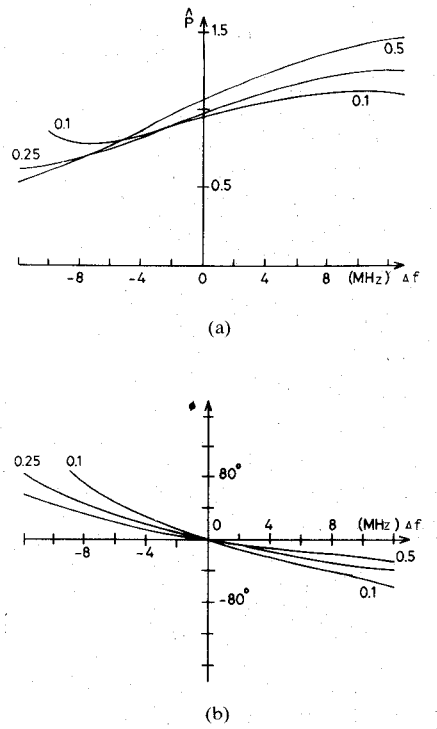

Fig. 3. Injection-locking characteristics with B_v added. ($\hat{G}_0 = 2.36$, $\hat{G}_v = 1.18$, $\hat{B}_0 = -2.16$, $\hat{B}_\omega = 1$, $\hat{B}_v = 1.83$.) (a) Amplitude characteristics. (b) Phase characteristics.

C. The Effect of the Coefficient B_v

The effect of the coefficient B_v on the Rieke diagram is to bend the equi-frequency loci. As to the injection-locking characteristics, B_v is closely related to the phase difference between the incident wave b and the emanating wave a. Even for a small-signal injection at the free-running frequency ω_0, $\phi \equiv \alpha - \beta$ is not equal to zero, as in the case of the Van der Pol oscillator. For an oscillator with parameters of $\hat{G}_0 = 2.36$, $\hat{G}_v = 1.18$, $\hat{B}_0 = -2.16$, $\hat{B}_\omega = 1$, $\hat{B}_v = 1.83$, the phases for input powers of $|\hat{b}|^2 = 0.1$, 0.25, and 0.5 are $\phi = -74°$, $-82°$, and $-92°$, respectively, because of the effect of B_v. But in Fig. 3(b), all loci are drawn to pass through the origin for convenience of comparison with the experiment.

When $|\hat{b}|^2 \to 0$, ϕ is given by (see Appendix II)

$$\phi = -\theta = -\arctan(B_v/G_v). \tag{14}$$

D. The Effect of the Coefficient $G_{\omega 2}(>0)$

Normally, the coefficient $G_{\omega 2}$ is positive. $G_{\omega 2}$ makes the injection-locking frequency range narrower, because the absolute value of negative conductance decreases as the frequency deviates from the free-running frequency. Generally speaking, the value of $\hat{G}_{\omega 2}$ is $0.0 \sim 0.4$ for electronic-tube oscillators, and $0.0 \sim 0.1$ for semiconductor oscillators. If $\hat{G}_{\omega 2} < 0.5$, we do not find so remarkable an effect on the injection-locking characteristics.

E. The Effect of the Coefficient $B_{\omega 2}$

The coefficient $B_{\omega 2}$ changes the intervals between equi-frequency loci on the Rieke diagram. As $|\hat{b}_{\omega 2}|$ becomes larger, the injection-locking frequency range becomes narrower asymmetrically.

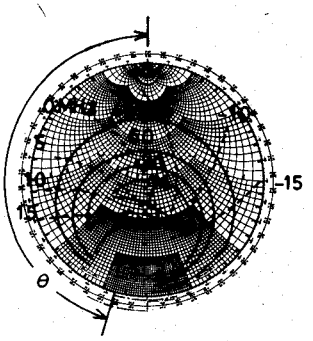

Fig. 4. Measured Rieke diagram of the Gunn oscillator 10GM081.

IV. Example

As an example, we investigated the injection-locking phenomena of the Gunn oscillator 10GM081 (free-running frequency $f_0 = 8848$ MHz). From the Rieke diagram of Fig. 4, the coefficients of (13) are determined as [4]

$$\hat{G}_0 = 2.36, \quad \hat{G}_\omega = -0.00267, \quad \hat{G}_v = 1.18, \quad \hat{G}_{\omega 2} = 0.0258$$
$$\hat{B}_0 = -1.078, \quad \hat{B}_\omega = 1, \quad \hat{B}_v = 0.916, \quad \hat{B}_{\omega 2} = 0.0264$$

where the normalization factors are $Y_0 = 0.002$ [S], $G_v = 0.735 \times 10^{-4}$[$S/V^2$], and $B_\omega = 0.206 \times 10^{-3}/2\pi$[$S$/MHz] $= 0.328 \times 10^{-4}$[S/MHz]. From the consideration of the previous results, we can neglect the coefficients G_ω, $G_{\omega 2}$, and $B_{\omega 2}$ so as to simplify the equation. Using those coefficients, we have reproduced the Rieke diagram of Fig. 5. Comparing Fig. 4 with Fig. 5, we see that the mathematical expression of the oscillator characteristics is fairly satisfactory. Fig. 6 shows the injection-locking characteristics of the Gunn oscillator 10GM081. Using the values

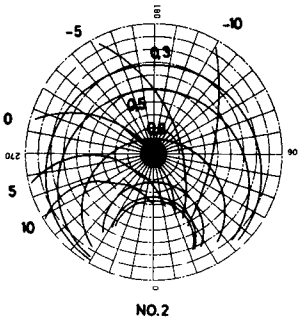

Fig. 5 Reproduced Rieke diagram. ($\hat{G}_0 = 2.36$, $\hat{G}_v = 1.18$, $\hat{B}_0 = -1.078$, $\hat{B}_\omega = 1$, $\hat{B}_v = 0\,916$.)

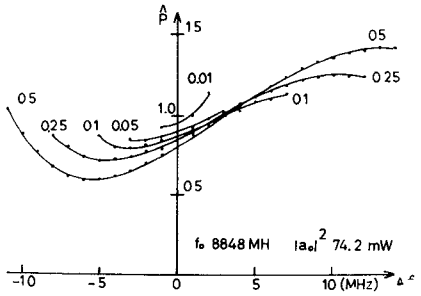

(a)

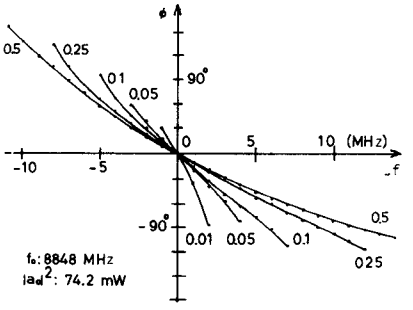

(b)

Fig. 6. Measured injection-locking characteristics of the Gunn oscillator 10GM081. (a) Amplitude characteristics (b) Phase characteristics.

(Y_n, B_v, and Y_v) which are determined from the Rieke diagram, we can predict the injection-locking characteristics, as is shown in Fig. 7. The computed result of Fig. 7 is in good agreement with the measured characteristics of Fig. 6. In Fig. 7, the phase differences due to the effect of B_v corresponding to $|\hat{b}|^2 = 0.1$, 0.25, and 0.5 are $\phi = -50°$, $-58°$, and $-68°$, respectively. All loci are, however, drawn to go through the origin for easy comparison with the experiment. When $|\hat{b}|^2 \to 0$, $\phi = -38°$ from (14).

If we employ the Van der Pol oscillator model, the amplitude characteristics are always symmetric with respect to frequency, and calculated values do not agree as well with the experiment.

V. Conclusion

In this paper, we investigated the relationship between the loading and the injection-locking characteristics of microwave oscillators by making use of (1). A close agreement between observed and calculated results was obtained.

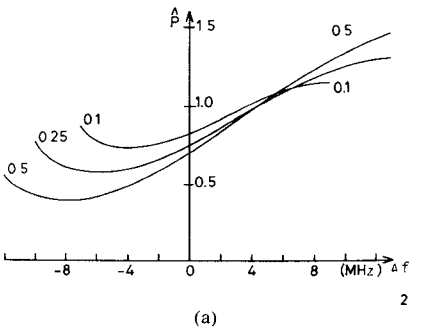

(a)

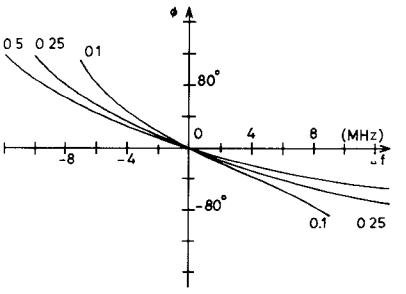

(b)

Fig. 7. Reproduced injection-locking characteristics of the Gunn oscillator 10GM081. ($\hat{G}_0 = 2.36$, $\hat{G}_v = 1\,18$, $\hat{B}_0 = -1.078$, $\hat{B}_\omega = 1$, $\hat{B}_v = 0.916$.) (a) Amplitude characteristics. (b) Phase characteristics.

Appendix

A. Stability Criterion

Let us consider an equation expressed as

$$\frac{dz}{dt} = F(z, z^*), \qquad z = x(t) + jy(t). \tag{A1}$$

We obtain the variational equation

$$\frac{d\delta x}{dt} = \frac{\partial F_r}{\partial x}\delta x + \frac{\partial F_r}{\partial y}\delta y$$

$$\frac{d\delta y}{dt} = \frac{\partial F_i}{\partial x}\delta x + \frac{\partial F_i}{\partial y}\delta y \tag{A2}$$

where $F_r = \mathrm{Re}\{F(z, z^*)\}$, $F_i \equiv \mathrm{Im}\{F(z, z^*)\}$, and the superscript * denotes the complex conjugate. We have an eigenvalue equation for the variational equation

$$\lambda^2 - \left(\frac{\partial F_r}{\partial x} + \frac{\partial F_i}{\partial y}\right)\lambda + \begin{vmatrix} \partial F_r/\partial x & \partial F_r/\partial y \\ \partial F_i/\partial x & \partial F_i/\partial y \end{vmatrix} = 0. \tag{A3}$$

From Routh–Hurwitz' criterion, we get the stability condition

$$\frac{\partial F_r}{\partial x} + \frac{\partial F_i}{\partial y} < 0 \tag{A4}$$

$$\begin{vmatrix} \partial F_r/\partial x & \partial F_r/\partial y \\ \partial F_i/\partial x & \partial F_i/\partial y \end{vmatrix} > 0. \tag{A5}$$

Noting the relation

$$\frac{\partial F}{\partial x} = \frac{\partial z}{\partial x}\frac{\partial F}{\partial z} + \frac{\partial z^*}{\partial x}\frac{\partial F}{\partial z^*} = \frac{\partial F}{\partial z} + \frac{\partial F}{\partial z^*} \tag{A6}$$

$$\frac{\partial F}{\partial y} = \frac{\partial z}{\partial y}\frac{\partial F}{\partial z} + \frac{\partial z^*}{\partial y}\frac{\partial F}{\partial z^*} = j\frac{\partial F}{\partial z} - j\frac{\partial F}{\partial z^*} \tag{A7}$$

we can rewrite (A4)

$$\frac{\partial F_r}{\partial x}+\frac{\partial F_i}{\partial y}=\left(\frac{\partial F_r}{\partial z}+\frac{\partial F_r}{\partial z^*}\right)+j\left(\frac{\partial F_i}{\partial z}-\frac{\partial F_i}{\partial z^*}\right)$$
$$=\frac{\partial F}{\partial z}+\frac{\partial F^*}{\partial z^*}=2\mathrm{Re}\frac{\partial F}{\partial z} \tag{A8}$$

and (A5)

$$\begin{vmatrix}\partial F_r/\partial x & \partial F_r/\partial y\\ \partial F_i/\partial x & \partial F_i/\partial y\end{vmatrix}=\begin{vmatrix}\partial F_r/\partial z+\partial F_r/\partial z^* & j\frac{\partial F_r}{\partial z}-j\frac{\partial F_r}{\partial z^*}\\ \partial F_i/\partial z+\partial F_i/\partial z^* & j\frac{\partial F_i}{\partial z}-j\frac{\partial F_i}{\partial z^*}\end{vmatrix}$$
$$=2j\begin{vmatrix}\partial F_r/\partial z & \partial F_r/\partial z-\partial F_r/\partial z^*\\ \partial F_i/\partial z & \partial F_i/\partial z-\partial F_i/\partial z^*\end{vmatrix}$$
$$=-2\begin{vmatrix}\partial F/\partial z & \partial F/\partial z^*\\ \partial F_i/\partial z & \partial F_i/\partial z^*\end{vmatrix}$$
$$=\begin{vmatrix}\partial F/\partial z & \partial F/\partial z^*\\ \partial F^*/\partial z & \partial F^*/\partial z^*\end{vmatrix}. \tag{A9}$$

From the above results, the concise expression for stability criterion (10) is deduced.

B. The Relation between the Coefficient B_v and the Locked Phase Difference θ

Let the oscillator admittance be given by

$$Y(j\omega,|V|^2)=Y_n+jB_\omega\,\Delta\omega+Y_v|V|^2 \tag{A10}$$

and let us derive the microwave injection-locking equation.

In the case of a small signal $|b|$, we obtain from (3)–(5) and (8) [3]

$$\left[\frac{Y_{|V_0|}}{\sqrt{Y_0}}\{\Delta|a|+|b|\cos(\beta-\alpha)\}+Y_{j\omega}\cdot(j\Delta\omega+d/dt)\right]a=2Y_0\cdot b. \tag{A11}$$

If the oscillator is adjusted to produce the maximum output power at the free-running state ($\hat{G}_0=2$), the real part of (A11) becomes zero [3]. Noting that $a^{-1}\,da/dt=|a|^{-1}d|a|/dt+jd\alpha/dt$, the imaginary part gives

$$\frac{d\alpha}{dt}=\frac{2Y_0}{B_\omega}\sqrt{1+(B_v/G_v)^2}\left|\frac{b}{a}\right|\sin(\beta-\alpha-\theta)-\Delta\omega \tag{A12}$$

where

$$\theta=\arctan(B_v/G_v)$$

C. Geometrical Meaning of the Locking Phase Difference

$$\theta=\arctan(B_v/G_v)$$

We assume that the oscillator admittance is given by (A10) and that the oscillator is adjusted to generate the maximum output power in the free-running state ($G_0=2Y_0$). When a load $Y_L=G_L+jB_L$ is connected to the oscillator, we have

$$Y(j\omega,|V|^2)+Y_L=0. \tag{A13}$$

If the load is matched to the transmission line ($Y_L=Y_0$), the above equation becomes identical to (4).

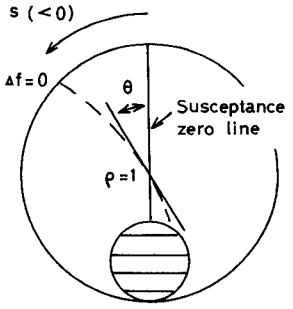

Fig. 8. Geometrical meaning of the injection-locking phase-difference θ on the Rieke diagram.

($\tan\theta=B_v/G_v=-S$, when $G_0=2Y_0$.)

We denote the normalized susceptance by S, on which the locus $\Delta\omega=0$ crosses the zero conductance locus (peripheral circle). Noting that $Y_L=jSY_0$, (A13) becomes

$$Y(j\omega_0,|V_1|^2)+jSY_0=0. \tag{A14}$$

Eliminating $B_0,|V_0|^2$, and $|V_1|^2$ from (4) and (A14), we obtain

$$\tan\theta=B_v/G_v=-S.$$

By the principle of conformal mapping, θ is equal to the angle between the locus of $\Delta\omega=0$ and the zero-susceptance line at the point of the matched load ($Y_L=Y_0$), as is shown in Fig. 8.

ACKNOWLEDGMENT

The authors would like to thank H. Mizuno of Nippon Denso Co. Ltd. for his aid in the experiments.

REFERENCES

[1] R. Adler, "A study of locking phenomena in oscillators," *Proc. IRE*, vol. 34, pp. 351–357, 1946.
[2] K. Kurokawa, *An Introduction to the Theory of Microwave Circuits*. New York: Academic Press, 1969.
[3] M. Nakajima and J. Ikenoue, "Locking phenomena in microwave oscillator circuits," *Int. J Electron*, vol. 44, pp. 465–472, 1978.
[4] K. Fukumoto, M. Nakajima, and J. Ikenoue, "Mathematical representation of microwave oscillator characteristics by use of the Rieke diagram," *IEEE Trans. Microwave Theory Tech.*, vol. MTT-31, pp. 954–959, 1983.

A New Cylindrical Electron Gun for Low-Power Tunable Gyrotrons with High Magnetic Compression Ratios

J. Y. L. MA

***Abstract*—Because of the high magnetic compression ratio required, electrons in the Sydney University tunable gyrotron undergo multiple reflections before entering the resonant cavity. This results in unstable and**

Manuscript received April 3, 1984; revised November 19, 1984. This work was supported in part by the Australian Research Grants Scheme, the Australian Institute of Nuclear Science and Engineering, the Radio Research Board, the University of Sydney, and the Science Foundation for Physics.

The author is with the Wills Plasma Physics Department, School of Physics, University of Sydney, N.S.W. 2006, Australia.

0018-9480/85/0400-0323$01.00 ©1985 IEEE